ACS APPLIED MATERIALS & INTERFACES

Research Article

www.acsami.org

Synthesizing a Healable Stretchable Transparent Conductor

Junpeng Li,[†,‡] Shuhua Qi,[‡] Jiajie Liang,[†] Lu Li,[†] Yan Xiong,[†] Wei Hu,[†] and Qibing Pei*[,†]

[†]Department of Materials Science and Engineering, Henry Samueli School of Engineering and Applied Science, University of California, Los Angeles, California 90095, United States

[‡]Department of Applied Chemistry, School of Science, Northwestern Polytechnical University, Xi'an Shaanxi, 710072, PR China

Supporting Information

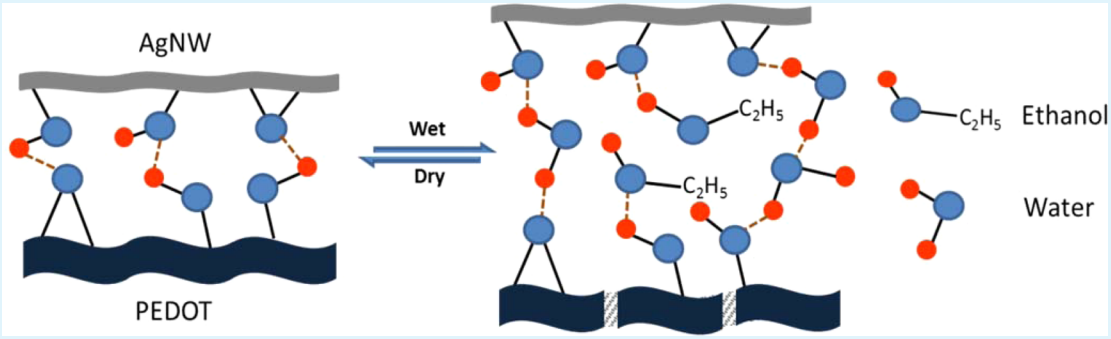

ABSTRACT: We report the first demonstration of a healable stretchable transparent electrode comprising a silver nanowire (AgNW) network and poly(3,4-ethylenedioxythiophene):polystyrenesulfonate (PEDOT) hybrid layer in the surface of a Diels–Alder elastomer substrate. The thin PEDOT layer solders the silver nanowires and confines the nanowire network in the substrate surface. The bonding between the nanowires and PEDOT is tuned via ethanol–water wetting, which allows for large-strain prestretching of the AgNW network. The composite electrode prepared via such a wetting and prestretching treatment has a figure-of-merit sheet resistance of 15 ohm/sq with 78% transmittance at 550 nm and can be stretched by 100% strain. Damages caused by razor blade cutting on the conductive surface could be healed, and the damaging-healing could be repeated for three times at the same location. The healed electrode exhibits similar resistance–strain response as the fresh electrode because of the PEDOT layer being capable of circumventing broken nanowire sites. Fatigue-induced damages after 100 cycles of 60% strain can also be healed by simple heating.

KEYWORDS: *stretchable composite electrode, healable, transparent, silver nanowire, PEDOT:PSS*

INTRODUCTION

Transparent electrode possessing elastomeric deformability is a key component in the next generation of flexible electronic devices, such as smart skin,[1] stretchable display,[2−4] energy-related devices,[5] stretchable solar cells,[6−8] stretchable integrated circuits,[9] and elastomeric organic transistors.[10,11] Repeated large-strain deformation inevitably causes fatigue, crack formation, and loss of local or global electrical conduction. There have been considerable reports of healable composite conductors to extend device lifetime,[12] improve fault-tolerance,[13] and obtain materials recyclability.[14] Certain Diels–Alder (DA) cycloaddition polymers have been developed capable of performing multiple damage-healing events at the same location, thanks to the reversibility of the DA reaction.[15] We previously reported a healable transparent conductor based on silver nanowires (AgNW) embedded in the surface of a DA copolymer substrate.[16] While being flexible (bendable), the AgNW/DA healable composite electrode is relatively rigid and lacks elastomeric deformability.

So far, healable stretchable transparent electrode has not been attainable, as there are fundamental challenges to accomplish transparency, conduction, elastomeric deformability and healability all in the same material. Elastomeric electrodes have typically been fabricated by either transferring a conductive percolation network onto an in situ formed polymer substrate,[4,8,17,18] or depositing conductors onto the surface of a preformed wavy, buckled or meshed elastomeric substrate.[6,10,19] Strong bonding between the conductive network and the substrate is necessary to carry out the transfer, avoid detachment of the conductive material during deformation or physical contact, such as a finger pressing, and maintain electrical conduction at high strain deformation. To maintain electrical conduction during stretching, the conductive network must elongate with and remain conformed on the substrate. On the other hand, the healing of a DA polymer substrate involves heating to break the DA bonds and soften the DA network to allow molecular or polymer chain motion to fill in the gap of a crack. During the molecular motion, AgNW could relocate and

Received: April 22, 2015
Accepted: June 10, 2015
Published: June 10, 2015

DOI: 10.1021/acsami.5b03482
ACS Appl. Mater. Interfaces 2015, 7, 14140−14149

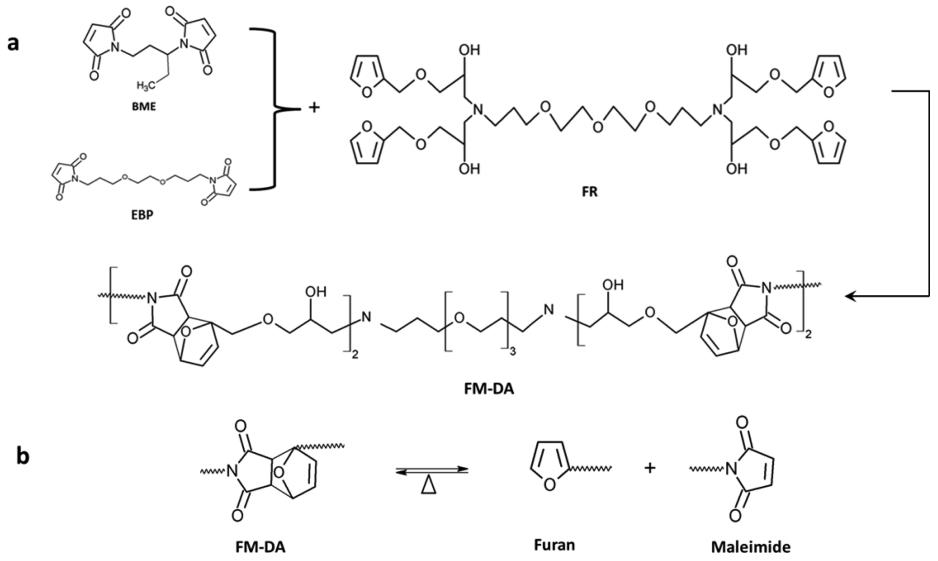

Figure 1. (a) Synthesis of the FM−DA copolymer elastomer. (b) Reversible DA reaction and retro-DA reaction between furan and maleimide.

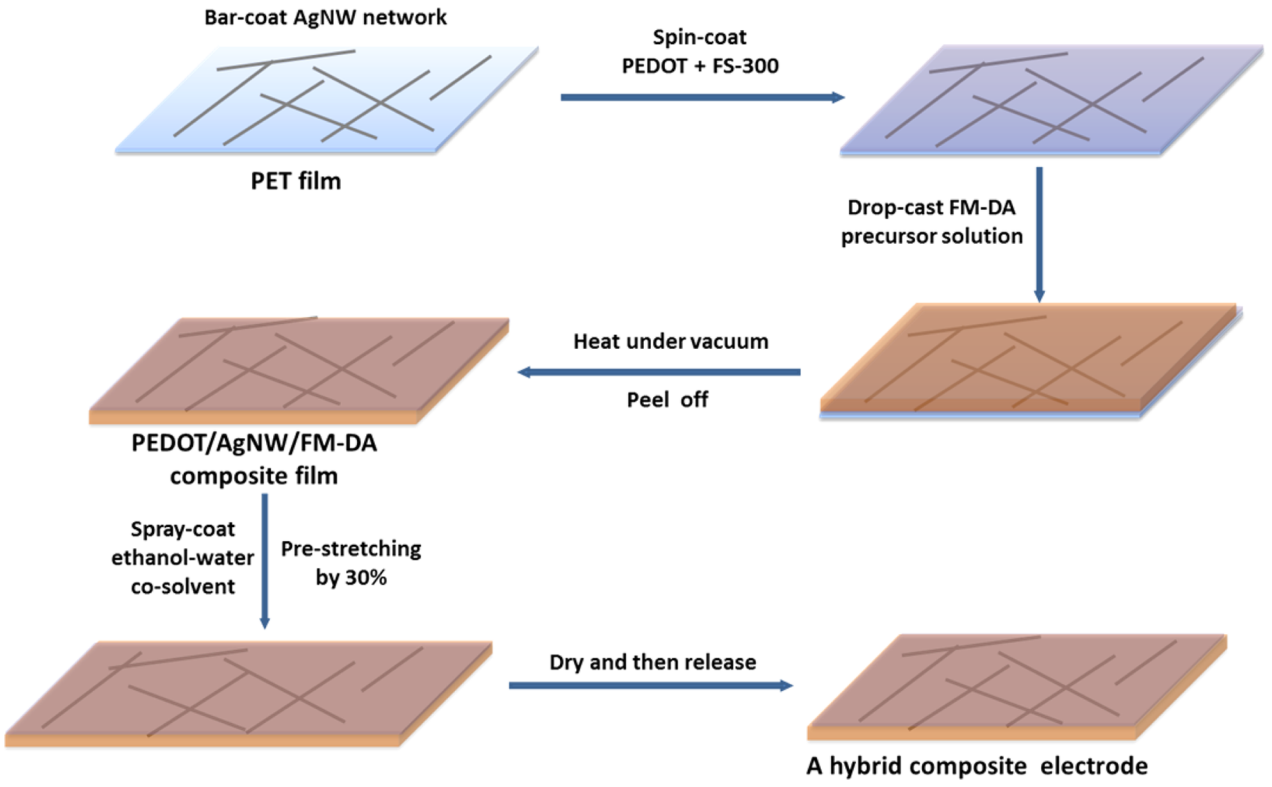

Figure 2. Schematic illustration of the fabrication of PEDOT/AgNW/FM−DA hybrid composite electrode.

thus disrupt the conduction network. In the case of rigid DA polymer substrate, this problem could be overcome by confining the AgNW network within an ultrathin layer of a non-DA polymer coated on the DA polymer substrate.[16]

Attempts to directly apply this approach to elastomeric composite electrode were not successful. We thus replaced the thin surface polymer layer with poly(3,4-ethylenedioxythiophene):polystyrenesulfonate (PEDOT), which has been widely used in AgNW-based transparent electrode for flexible and stretchable devices.[4,20−23] The PEDOT layer helps solder the nanowires and reduce internanowire resistance.[6,24−26] A conductive PEDOT layer modified with a fluorosurfactant shows no resistance change after 5000 cycles of 0% to 10% strain.[27]

Our objective is to modify the PEDOT layer as a tunable binder for the nanowires: proper wetting of the PEDOT coating could lose the bonding strength with the AgNWs, allow slippage of the nanowires during stretching, and thus avoid fracture of the nanowires at large deformation. Large-strain prestretching could therefore be introduced to enhance stretchability. The dried PEDOT layer could strongly bind nanowires and confine the nanowires on the surface of a DA polymer substrate during DA precursor curing and substrate healing. Here, we report that such a PEDOT/AgNW/DA

DOI: 10.1021/acsami.5b03482
ACS Appl. Mater. Interfaces 2015, 7, 14140−14149

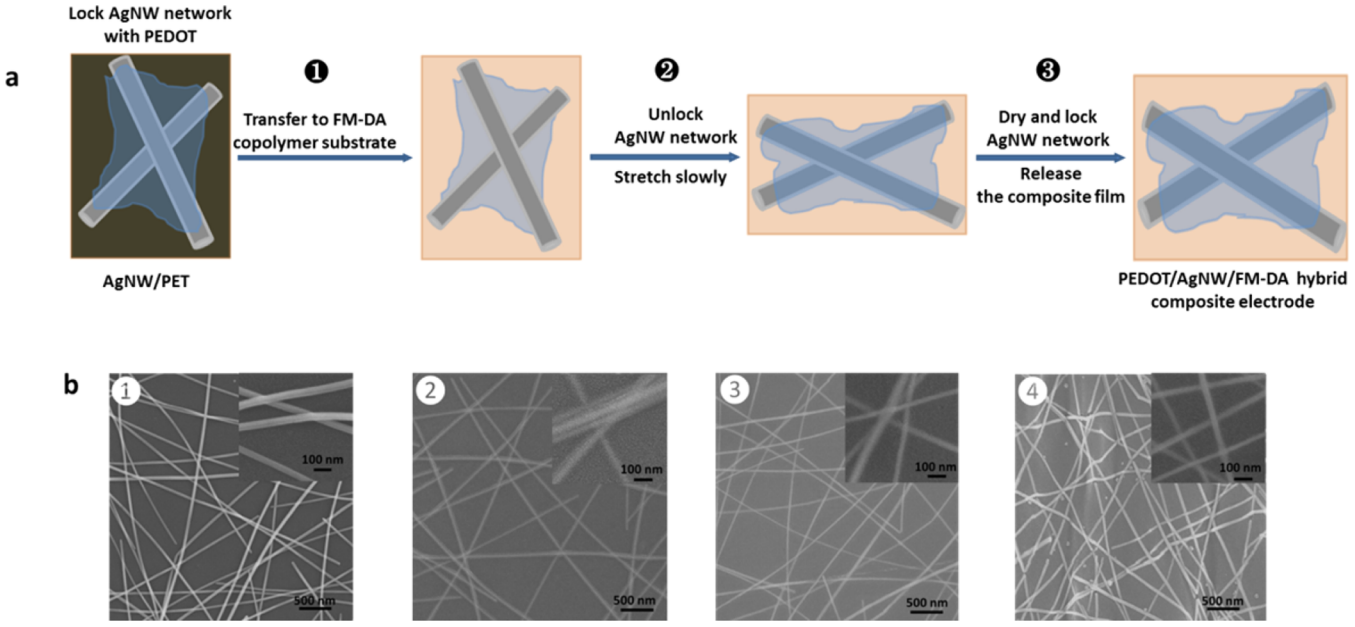

Figure 3. (a) Schematic illustration of AgNW network morphology during the fabrication of a hybrid composite electrode and (b) the corresponding SEM micrographs of the electrode surface: (1) AgNW network on PET release substrate without thermal annealing, (2) overcoated with PEDOT, (3) transferred onto FM−DA elastomer surface, and (4) the elastomeric composite electrode after 30% prestretching. Insets: Blown-up SEM images to show the AgNW junctions.

copolymer composite electrode exhibits elastomeric stretchability within the prestretching ratio. Beyond the prestretching ratio, the conductive PEDOT coating can offset the resistance increase caused by AgNW network breakage. Damages caused by fatigue after repeated stretching could be healed by simple heating at 100 °C. A survey of previous reports shown Supporting Information Table S1 indicates that this work represents the first healable elastomeric transparent electrode.

RESULTS AND DISCUSSION

The transparent DA elastomeric polymer, with the acronym FM−DA, was synthesized through a reversible DA cycloaddition reaction of three cross-coupling comonomers: a furan oligomer and two maleimide monomers with the acronyms of FR, BME, and EBP, respectively, as shown in Figure 1a. See Method for the preparation of the healable elastomer. FR, BME, and EBP were synthesized according to our previously published method,[15] Kossmehl's work,[28] and Chen's work,[29] respectively.

The retro-DA reaction occurs efficiently upon heating as illustrated in Figure 1b. Because of the reversibility of the DA reaction, cutting or crack across the copolymer film surface can heal upon heating at 100 °C. The healing progress of a blade-cut damage is shown in Supporting Information Figure S1. Most cut wound healed in 5 min. After 30 min, the wound was fully healed.

Figure 2 illustrates the fabrication of a healable stretchable transparent hybrid composite electrode. The process begins with bar-coating an AgNW solution on a PET release substrate, followed by spin-coating a water solution of PEDOT and FS-300. A solution of the FM−DA elastomer precursor is deposited and cures at 70 °C under vacuum for 6 h to form a healable composite film. The composite film is peeled off the PET release substrate. The AgNW percolation network is transferred into the surface of the copolymer film. Then a cosolvent containing 80% ethanol and 20% water by volume is spray-coated on the conductive surface of the composite film; the composite film is slowly stretched by 30% linear strain while the surface is kept wet. Finally, the composite film is allowed to dry and then released to free-standing.

The morphology of the AgNW network during composite electrode fabrication is illustrated in Figure 3a. The conductive AgNW network is locked together on the PET release film by dry PEDOT coating, then completely transferred to the surface of FM−DA shown in Support Information Figure S2. While solvent wetting the PEDOT layer unlocks the AgNW network, the composite electrode is stretched. The AgNW network could slip along the stretching direction. As the PEDOT layer is dried, the AgNW network is relocked on the stretched FM−DA surface.

Figure 3b(1) shows AgNW network on PET substrate. The PEDOT coating could conform onto the nanowires and wrap around the nanowire-nanowire junctions to reduce internanowire contact resistance as shown in Figure 3b(2).[30] Note that without a layer of PEDOT, the AgNW network on PET film would be immersed in the precursor solution during the curing of the FM−DA copolymer substrate at 70 °C for 6 h. The polymer precursor solution has low viscosity, so the nanowires could relocate due to thermodynamics or Brownian motion. Segments of AgNW could submerge deep into the copolymer substrate, and distribute below the substrate surface as shown in Supporting Information Figure S3a. The surface resistance would be high. With the use of a PEDOT layer, the nanowires are confined in the PEDOT layer on the surface of FM−DA copolymer substrate, as shown in Supporting Information Figure S3b, and maintains low sheet resistance. For instance, by transferring the same coating density of AgNW from PET release substrate, the composite electrode comprising the PEDOT layer had a sheet resistance of 15 ohm/sq, whereas the composite electrode without this intermediate layer showed a sheet resistance of 320 ohm/sq (see data in Supporting Information Figure S4). Figure 3b3 shows the SEM image of a

DOI: 10.1021/acsami.5b03482
ACS Appl. Mater. Interfaces 2015, 7, 14140−14149

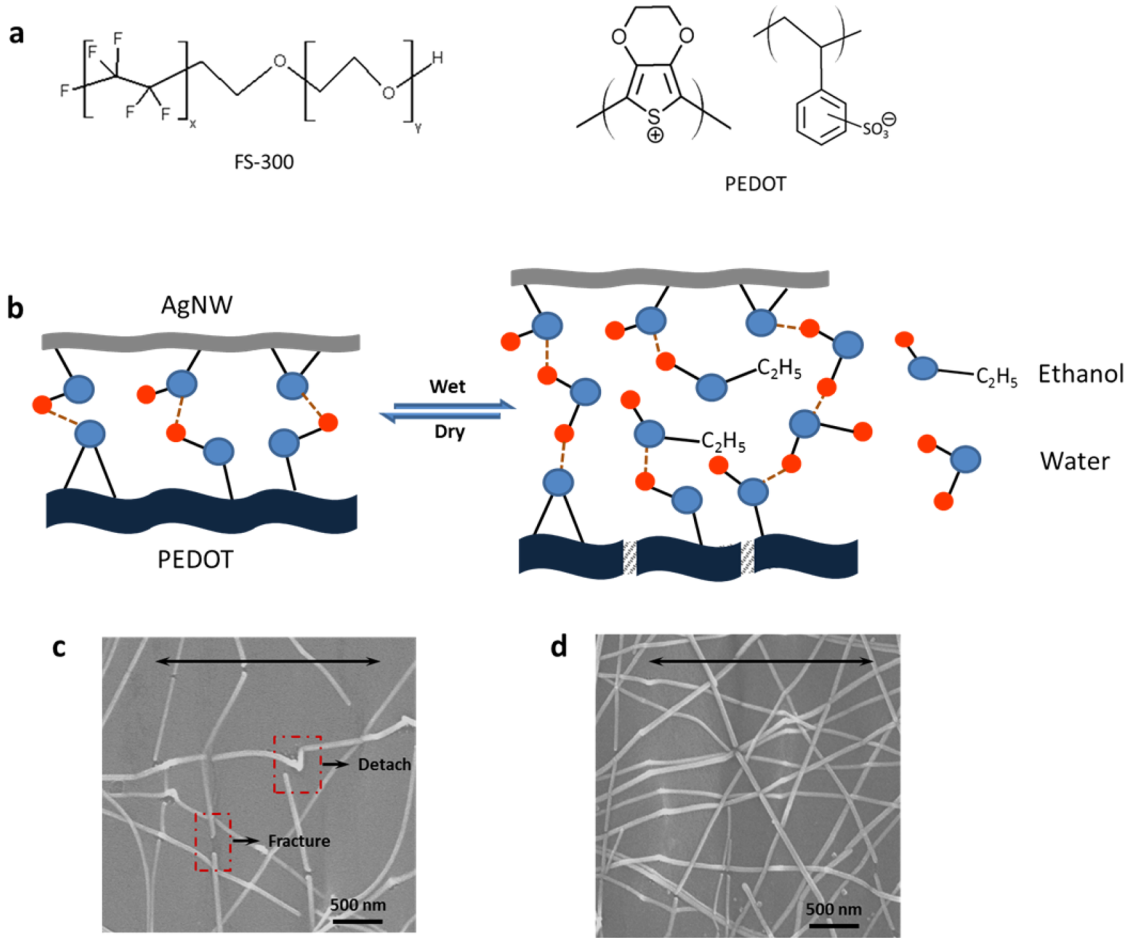

Figure 4. (a) Chemical structures of PEDOT and FS-300. (b) Schematic showing various hydrogen bonds between AgNW and dry PEDOT (left), and AgNW and wet PEDOT (right). The blue and red spheres represent oxygen and hydrogen atoms, respectively. (c, d) SEM images of relaxed composite electrodes after stretching up to 30%. During stretching, the composite films with a dry PEDOT layer (c) and a wet PEDOT layer (d). Arrows indicate stretching direction.

hybrid composite electrode after the first preparation step (Figure 3a1). AgNW network is embedded in the PEDOT layer on the surface of FM−DA copolymer substrate.

During the second step of the preparation, the hybrid composite film was stretched on a linear stage slowly; meanwhile, a cosolvent made of 80% ethanol and 20% water was spray-coating on the conductive surface. The PEDOT layer could be solved by the cosolvent[31,32] and become a loose paste, which "unlocked" the AgNW junctions, and also weakened the bonding strength between AgNW network and PEDOT. The unlocked AgNWs could slip in the PEDOT layer along the copolymer substrate surface. The AgNW percolation network structure thus rearranged along the tensile direction to accommodate to the elongation of the substrate. Finally, the stretched composite film was allowed to dry and then released from the linear stage. The AgNW conductive network was relocked firmly on the FM−DA substrate surface. The global conduction network should still be retained. The SEM image in Figure 3b4 shows the resulting composite electrode. AgNW network is wrapped by the PEDOT on copolymer substrate.

This "lock-unlock" processing can be explained by hydrogen bonding between AgNW and PEDOT. The fluorosurfactant FS-300 is used as an addictive to improve the wetting of PEDOT solution on AgNW surface and the FM−DA copolymer surface.[27,33] Their chemical structures are available in Figure 4a. FS-300 as an amphiphilic chemical with both fluorinated and ethylene glycol segments has the interaction with PEDOT. The ethylene glycol group enables chemical coupling with the AgNW surface via O−Ag bounding, and it is expected to improve the bonding strength between PEDOT and AgNW.[34−36]

The humidity-induced bonding release property of PEDOT/AgNW can be explained by examining the hydrogen bond network between hydroxyl and ether functional groups on FS-300, which can chemically absorb onto the surfaces of AgNW and PEDOT. In a dry situation, H-bond network is formed between Ag and PEDOT by the hydrogen and the oxygen atoms, which are covalently bonded to hydroxyl and ether functional groups from FS-300 illustrated in Figure 4b (left). AgNW adheres on the surface of PEDOT layer firmly by FS-300. Supporting Information Figure S5 shows the strong bonding of AgNW on the surface of PEDOT/FM−DA copolymer substrate. After 1000 cycles of adhesion-peeling, only 1 ohm/sq increase was measured. A hydrated hybrid PEDOT/AgNW layer displays various configurations of O−H bonds, as shown schematically in Figure 4b (right). H-bond network is dominated by bonds with water and ethanol molecules. The AgNW does not interact with PEDOT layer by FS-300; instead, their interaction is mediated by a network of H-bonded water and ethanol molecules. That is because water

DOI: 10.1021/acsami.5b03482
ACS Appl. Mater. Interfaces 2015, 7, 14140−14149

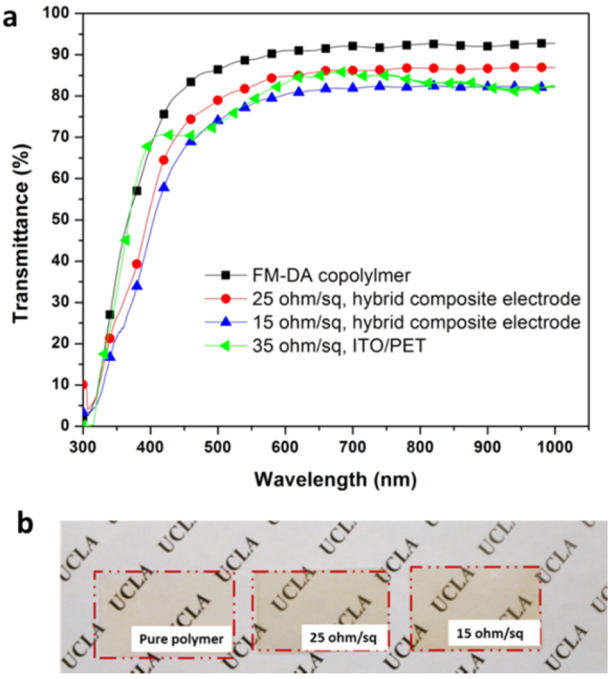

Figure 5. (a) Transmittance spectra of a FM−DA copolymer film, PEDOT/AgNW/FM−DA hybrid composite electrodes with specified sheet resistances. Data for a commercial ITO/PET film is also shown for comparison. All transmittance data are inclusive of substrate. The thickness of all films is 150 μm. (b) Optical photographs of FM−DA film and relative composite films.

and ethanol as polarized small molecules can penetrate into interspace, which ease the interface adhesion and render AgNW freedom within PEDOT layer. Additionally, PEDOT layer can be solved by the cosolvent of ethanol and water into segments, which benefits the slippage of hybrid PEDOT/AgNW layer along the copolymer substrate surface.

SEM images of PEDOT/AgNW/FM−DA composite electrodes after 30% strain without (Figure 4c) and with the PEDOT layer being wetted by ethanol/water during stretching (Figure 4d) show that when the PEDOT layer is dry, the nanowires are significantly fractured and partially detach from the substrate due to limited elongation of AgNW (Figure 4c). When the PEDOT layer is wetted with a sprayed ethanol−water cosolvent, the nanowires are unlocked from the confinement of the PEDOT binder, and can deform to large global strains via relative slides among the nanowires and against the substrate. Most of the nanowires remain intact. When the cosolvent is evaporated away, the PEDOT layer resumes a relatively rigid structure. As the substrate is allowed to relax to 0% strain, the mismatch of the stretchability between the copolymer substrate and the dried PEDOT would form a buckled surface morphology, with the AgNW network locked in the surface contour (Figure 4d). This buckling can prevent significant fracture of the nanowires when stretching.

In the remaining discussions, all composite films were fabricated by this processing involving the prestretching while the PEDOT layer was wetted.

The optical transmittance of a FM−DA copolymer film and its composite electrodes are displayed in Figure 5a. The transmittance at 550 nm is 89%, 82%, and 78% for the neat copolymer film, its composite electrodes with 25 ohm/sq and 15 ohm/sq sheet resistance, respectively. The visual transparency of the 25 ohm/sq composite electrode is comparable to the commercial ITO/PET film with 35 ohm/sq sheet resistance.

The conductive healing property of the composite electrodes was examined by razor blade-cutting on the conductive surface and measuring the recovery of the conductivity upon heating (see Figure 6a). A cut penetrated into the polymer substrate around 40 μm depth. The resistance of the composite electrode increased to infinity (cannot be measured by a multimeter). After healing at 100 °C for 3 min, 85 °C for 5 min, or 70 °C for 8 min, the resistance with an initial value of 15 ohm recovered to the final resistance of 18 ± 1, 19 ± 2, and 20 ± 2 ohm, respectively. The resistance recovery speed is much higher at high temperature due to the faster DA bond reconnection. The healing progress in SEM images is shown in Supporting Information Figure S6.

The healing can be repeated at the same location for multiple times as shown in Figure 6b. The resistance of a composite electrode with initial resistance of 15 ohm increased to an infinite value after each deliberate cutting. The resistance recovered to 18, 40, and 500 ohm after healing at 100 °C in 3 min after the first, second, and third cutting, respectively. This

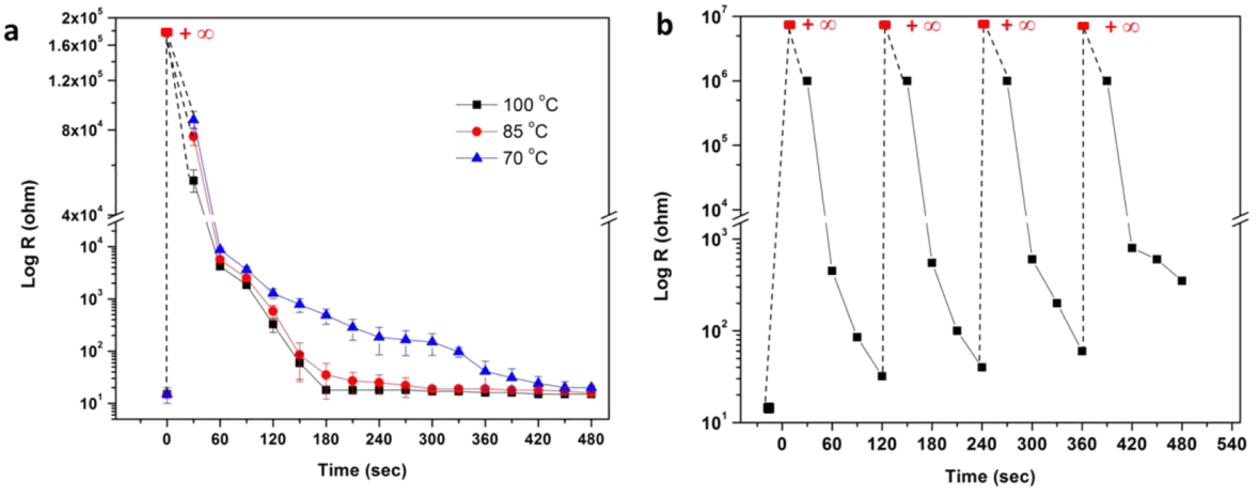

Figure 6. (a) Measured transient resistance of the hybrid composite electrodes during healing process at 100, 85, and 70 °C, respectively. (b) Multiple-healing cycles at the same location at 100 °C. All composite electrodes (20 mm × 20 mm × 0.15 mm) have an initial resistance of 15 ohm.

DOI: 10.1021/acsami.5b03482
ACS Appl. Mater. Interfaces 2015, 7, 14140−14149

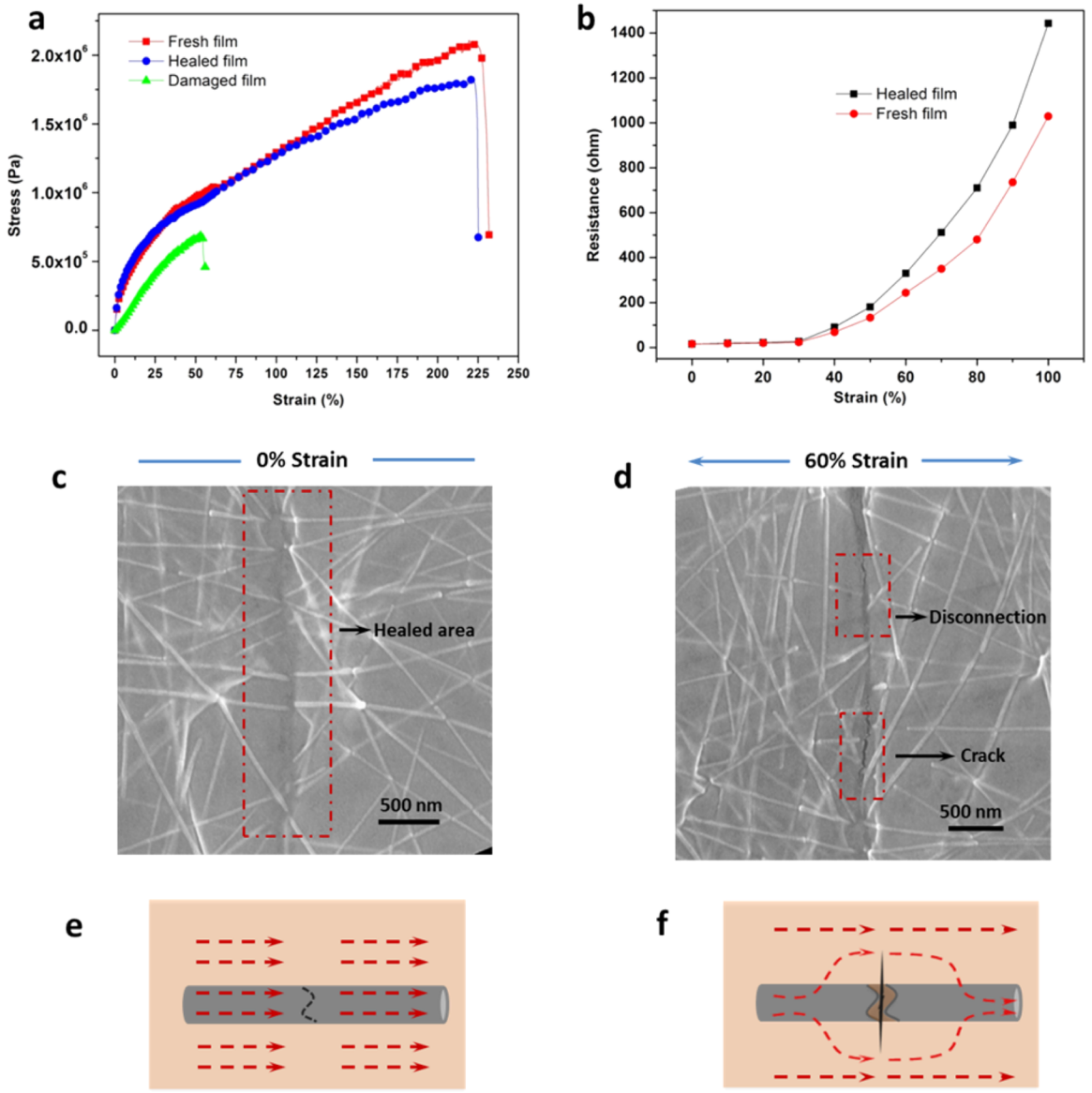

Figure 7. (a) Stress–strain curves of composite electrode freshly prepared, damaged by a blade-cutting, and healed at 100 °C for 3 min (sample area, 6 mm × 50 mm; strain speed, 1 mm/s). (b) Measured resistance of a fresh composite electrode and a healed composite electrode during stretching up to 100% strain (sample area, 7 mm × 10 mm; strain speed, 0.05 mm/s). (c, d) SEM images of a healed composite film (c) and under 60% strain (d). (e, f) Illustration of the conduction pathway on a healed composite film (e) and a healed composite film under 60% strain (f). All samples had an initial resistance of 15 ohm and 150 μm thickness.

declining healing efficiency in repeated cutting-healing at the same location is considered to be caused by the difficulty for AgNW network and conductive PEDOT layer to reconnect during healing of the substrate.

The mechanical healing performance was measured by stress and strain response shown in Figure 7a. On the surface with AgNW conductive network, blade cutting was made perpendicular to the tensile direction and roughly 40 μm depth. The maximum stress and strain at break of the damaged film were reduced dramatically. After healing at 100 °C for 3 min, the mechanical property of the healed sample was slightly weaker than the fresh film. The healing efficiency reached 97%.

To evaluate the robustness of the healed film, a composite film with initial resistance of 15 ohm was blade cut and then healed to a recovered resistance of 18 ohm. The healed film was stretched from 0% to 100% strain. The transient resistance with stretching is plotted in Figure 7b. Compared with the fresh film, the resistance of the healed was slightly high at given strains. The differences are 3 ohm and 68 ohm at 30% and 60% strains, respectively, which are considered small. Figure 7c and 7d show SEM images of a healed composite film, damaged by a deliberate cutting, under 0% and 60% strain, respectively. After healing, the AgNW network and PEDOT layer are both brought together by the healing polymer. The surface conduction is recovered. The whole healing progress is shown in Support Information Figure S6. On a healed film, charge transport could pass through the reconnected AgNW network and the conductive PEDOT layer. At 60% strain, AgNWs not properly healed are disconnected, and some cracks in the PEDOT layer are observed in Figure 7d. However, the composite film still retains a relative low resistance, 310 ohm versus 242 ohm for undamaged film at 60% strain. The PEDOT layer plays a key role in the high mendability: while PEDOT is not as conductive as the nanowires, it could offset

DOI: 10.1021/acsami.5b03482
ACS Appl. Mater. Interfaces 2015, 7, 14140–14149

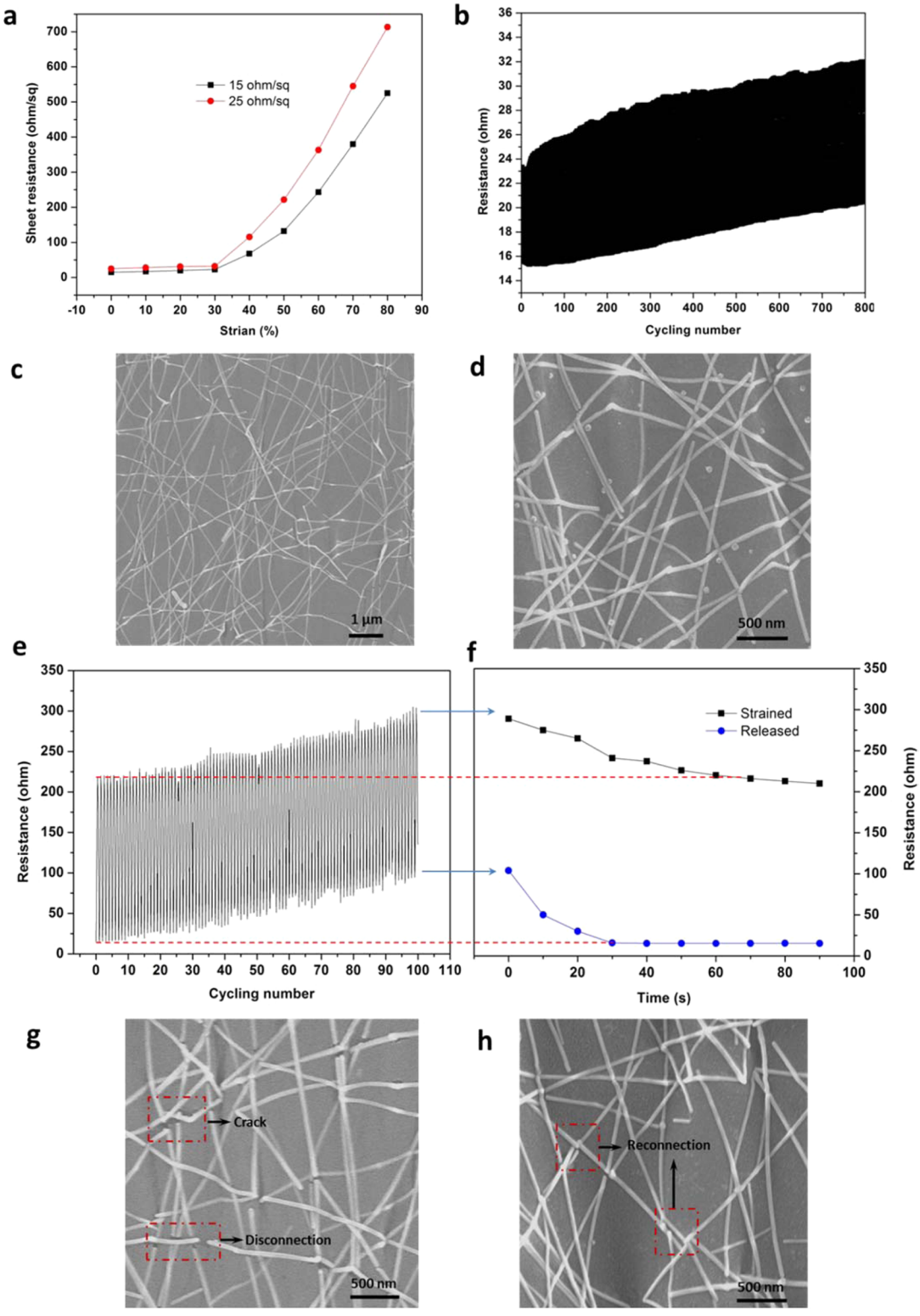

Figure 8. (a) Sheet resistance of composite electrodes with increasing strain (sample area, 7 mm × 10 mm). (b) Transient resistance measured during 800 cycles of stretching-relaxing between 0% and 30% strains for a 15 ohm/sq composite electrode (sample area, 5 mm × 5 mm; stretch speed, 0.05 mm/s). (c, d) SEM images of the composite film after 800 cycles of stretching-relaxing. (e) Resistance evolution of the composite film during 100 cycles of stretching-relaxing between 0% and 60% strains, and (f) evolution of the baseline and peak resistances during healing at 100 °C without strain applied. SEM images of (g) the composite film after 100 cycles of stretching-relaxing and (h) after healing at 100 °C, 70 s.

the resistance increase caused by the microcosmic gap between fractured AgNWs. Figure 7e and 7f illustrate the conductive pathway of a healed composite film with 0% strain and 60% strain, respectively. At 60% strain, conductive pathway would detour the disconnected AgNWs via the neighboring PEDOT area.

The sheet resistance changes of the 15 and 25 ohm/sq composite films with increasing strain up to 80% are shown in

DOI: 10.1021/acsami.5b03482
ACS Appl. Mater. Interfaces 2015, 7, 14140−14149

Figure 8a. Sheet resistances increased in two phases: from 0% to 30% strain, within the prestretching ratio, the increases in sheet resistance were small, and sheet resistances at 30% strain were 21 and 32 ohm/sq, respectively; from 30% to 80%, beyond the prestretching ratio, sheet resistance increased steadily. At 80% strain, sheet resistances were 480 ohm/sq and 680 ohm/sq, respectively.

The resistance evolution of the 15 ohm composite electrode during 800 cycles of continuous stretching-relaxing between 0 and 30% strains is shown in Figure 8b. With an initial resistance of 15 ohm, the peak resistance (at 30% strain) increased from 21 ohm to 25.5 ohm after the first 100 cycles, and to 32 ohm after the subsequent 700 cycles. The baseline resistance (at 0% strain) also increased slowly to 15.5 ohm after 100 cycles, and to 20.3 ohm in the subsequent 700 cycles. After 800 cycles of stretching-relaxing, the dense AgNW network appears intact. Without obvious substrate cracks or AgNW fractures are shown in Figure 8c and 8d.

Cyclic testing was also done between 0 and 60% strains as shown in Figure 8e. The peak resistance and the baseline resistance increased to 290 and 90 ohm, respectively, in 100 cycles. The resistance increase could be reversed by heating at 100 °C as shown in Figure 8f. The peak resistance and baseline resistance were restored in 70 and 30 s, respectively. The healed electrode is comparable as the fresh one. This indicates the fatigue in the composite electrode caused by repeated stretching could be healed.

SEM imaging was carried out to further examine the surface morphology of the composite electrode. After 100 cycles of stretching-relaxing between 0% and 60% strain, tiny substrate cracks and AgNW fractures have occurred on the composite surface (Figure 8g). These are attributed to the limited elongation of the nanowire network and the PEDOT, less than 60% strain. The aforementioned bonding strength among AgNW, PEDOT and the DA copolymer substrate prevents slippage of the nanowires across the substrate surface, and thus leads to AgNW fractures at large strains. However, the resistance still retains fairly low value, thanks to the conductive PEDOT layer. Figure 8h shows that the broken nanowires are reconnected as a result of the healing treatment.

CONCLUSIONS

In summary, a transparent stretchable conductor has been prepared comprising an AgNW network and PEDOT layer on the surface of a healable elastomeric copolymer substrate. The conductive PEDOT layer was introduced as a binder to "solder" the nanowire junctions for the AgNW network to lower the nanowire junction resistance, and confine the AgNW network to the surface of the healable elastomer substrate. The bonding between the nanowires and PEDOT could be tuned by wetting the PEDOT layer with ethanol–water, and large-strain prestretching could be done without fracturing the nanowires when the PEDOT layer was kept wet. The resulting hybrid composite film behaved like a typical elastomer with high surface conductivity. The initial sheet resistance of this composite electrode with 15 ohm/sq increased to 21 ohm/sq at 30% strain. After 800 cycles of stretching between 0 and 30% strain, the resistance increased from 15 to 20.3 ohm. The composite electrode could also be stretched beyond the prestretching ratio. After 100 cycles of stretching between 0% and 60% strain, the composite film is still as conductive as ITO/PET. Microcosmic damage induced by large-strain cyclic stretching was healed by heating at 100 °C for 70 s thanks to the reversible Diels–Alder cycloaddition reaction in the substrate. The use of PEDOT as the binder for the AgNW network is the key to the retention of high conductivity: conduction across broken nanowires could be circumvented via neighboring PEDOT area.

METHODS

Synthesis of the Healable Copolymer Film. A total of 0.25 g of BME and EBP with a weight ratio of 6:4 was fully dissolved into 2 mL of cyclopentanone. FR (0.19 g) was then added into the solution, and the mixture was sonicated until a clear solution was obtained. The solution was drop-cast on a clean PET substrate and polymerized at 70 °C for 6 h in vacuum.

Preparation of the Healable Elastomeric Transparent PEDOT/AgNW/FM–DA Hybrid Composite Electrode. AgNW was synthesized with an average diameter between 25 and 35 nm, and average length between 10 and 20 μm. A dispersion of AgNW (concentration of 1.5 mg/mL) in isopropanol and methanol (volume ratio, 1:2) was coated on PET substrate using a Meyer rod (RD Specialist). A water solution of 60% fresh PEDOT (Clevios PH1000, a 1:2.5 mixture of PEDOT and PSS) and 0.3% Zonyl FS-300 was spin-cast onto the AgNW network. After it was dried at 70 °C for 5 min, a solution of BME, EBP, and FR in cyclopentanone, similar to the preparation of a healable copolymer film, was drop-cast onto the PEDOT layer. The healable comonomers in solution subsequently copolymerized at 70 °C under vacuum for 6 h. The healable composite film was peeled off the PET substrate. Then the composite film was mounted on a motorized linear stage. The conductive surface was wet by spray-coating a mixture of 80% ethanol–20% water, and the composite electrode was stretched to 30% strain at a rate of 0.001 mm/s. Finally, the composite film was dry in room temperature and released to free-standing.

Characterization. The stretching and relaxing tests were performed on a motorized linear stage with a built-in controller (Zaber Technology). A Keithley 2000 digital multimeter was used to monitor resistance changes. Strain and resistance data were recorded via a custom-made Lab View code. All measurements were carried out at room temperature. Transmittance spectra were recorded on a Shimadzu UV-1700 spectrophotometer. Scanning electron microscopic images were taken using a JSM-6700F FE-SEM.

ASSOCIATED CONTENT

Supporting Information

Comparison of various healable conductors, healing progress at different time intervals, AgNW network on PET release substrate, PET release substrate after AgNW network was transferred, distribution of AgNW in a surface of the FM–DA copolymer substrate, SEM images of AgNW embedded in FM–DA copolymer film and the cross-section of the composite, illustration of AgNW distribution into FM–DA matrix, SEM images and illustration of the composite film comprising PEDOT layer, sheet resistance of composite electrodes without or with a PEDOT layer, sheet resistance of a composite film with PEDOT versus repeated cycles of adhesion and peeling, and SEM images of a composite electrode surface during a healing process. The Supporting Information is available free of charge on the ACS Publications website at DOI: 10.1021/acsami.5b03482.

AUTHOR INFORMATION

Corresponding Author

*E-mail: qpei@seas.ucla.edu.

Notes

The authors declare no competing financial interest.

DOI: 10.1021/acsami.5b03482
ACS Appl. Mater. Interfaces 2015, 7, 14140–14149

■ ACKNOWLEDGMENTS

The work reported here was supported by Air Force Office of Scientific Research (FA9550-12-1-0074, Dr. Charles Lee). J.L. acknowledges support by the China Scholarship Council Program.

■ REFERENCES

(1) Kim, D.-H.; Lu, N.; Ma, R.; Kim, Y.-S.; Kim, R.-H.; Wang, S.; Wu, J.; Won, S. M.; Tao, H.; Islam, A.; Yu, K. J.; Kim, T.-i.; Chowdhury, R.; Ying, M.; Xu, L.; Li, M.; Chung, H.-J.; Keum, H.; McCormick, M.; Liu, P.; Zhang, Y.-W.; Omenetto, F. G.; Huang, Y.; Coleman, T.; Rogers, J. A. Epidermal Electronics. *Science* **2011**, *333*, 838−843.

(2) Song, J.; Kulinich, S. A.; Li, J.; Liu, Y.; Zeng, H. A General One-Pot Strategy for the Synthesis of High-Performance Transparent-Conducting-Oxide Nanocrystal Inks for All-Solution-Processed Devices. *Angew. Chem., Int. Ed.* **2015**, *54*, 462−466.

(3) Song, J.; Li, J.; Xu, J.; Zeng, H. Superstable Transparent Conductive Cu@Cu4Ni Nanowire Elastomer Composites against Oxidation, Bending, Stretching, and Twisting for Flexible and Stretchable Optoelectronics. *Nano Lett.* **2014**, *14*, 6298−6305.

(4) Liang, J.; Li, L.; Niu, X.; Yu, Z.; Pei, Q. Elastomeric Polymer Light-Emitting Devices and Displays. *Nat. Photonics* **2013**, *7*, 817−824.

(5) Hu, L.; Pasta, M.; La Mantia, F.; Cui, L.; Jeong, S.; Deshazer, H. D.; Choi, J. W.; Han, S. M.; Cui, Y. Stretchable, Porous, and Conductive Energy Textiles. *Nano Lett.* **2010**, *10*, 708−714.

(6) Lipomi, D. J.; Tee, B. C.; Vosgueritchian, M.; Bao, Z. Stretchable Organic Solar Cells. *Adv. Mater.* **2011**, *23*, 1771−1775.

(7) Yu, Z.; Li, L.; Zhang, Q.; Hu, W.; Pei, Q. Silver Nanowire-Polymer Composite Electrodes for Efficient Polymer Solar Cells. *Adv. Mater.* **2011**, *23*, 4453−4457.

(8) Yu, Z.; Zhang, Q.; Li, L.; Chen, Q.; Niu, X.; Liu, J.; Pei, Q. Highly Flexible Silver Nanowire Electrodes for Shape-Memory Polymer Light-Emitting Diodes. *Adv. Mater.* **2011**, *23*, 664−668.

(9) Kim, D.-H.; Ahn, J.-H.; Choi, W. M.; Kim, H.-S.; Kim, T.-H.; Song, J.; Huang, Y. Y.; Liu, Z.; Lu, C.; Rogers, J. A. Stretchable and Foldable Silicon Integrated Circuits. *Science* **2008**, *320*, 507−511.

(10) Chae, S. H.; Yu, W. J.; Bae, J. J.; Dinh Loc, D.; Perello, D.; Jeong, H. Y.; Quang Huy, T.; Thuc Hue, L.; Quoc, V.; Yun, M.; Duan, X.; Lee, Y. H. Transferred Wrinkled Al_2O_3 for Highly Stretchable and Transparent Graphene-Carbon Nanotube Transistors. *Nat. Mater.* **2013**, *12*, 403−409.

(11) Lee, S.-K.; Kim, B. J.; Jang, H.; Yoon, S. C.; Lee, C.; Hong, B. H.; Rogers, J. A.; Cho, J. H.; Ahn, J.-H. Stretchable Graphene Transistors with Printed Dielectrics and Gate Electrodes. *Nano Lett.* **2011**, *11*, 4642−4646.

(12) Yuan, W.; Hu, L. B.; Yu, Z. B.; Lam, T. L.; Biggs, J.; Ha, S. M.; Xi, D. J.; Chen, B.; Senesky, M. K.; Gruner, G.; Pei, Q. B. Fault-Tolerant Dielectric Elastomer Actuators Using Single-Walled Carbon Nanotube Electrodes. *Adv. Mater.* **2008**, *20*, 621−625.

(13) Li, Y.; Chen, S.; Wu, M.; Sun, J. Polyelectrolyte Multilayers Impart Healability to Highly Electrically Conductive Films. *Adv. Mater.* **2012**, *24*, 4578−4582.

(14) Wang, Q.; Mynar, J. L.; Yoshida, M.; Lee, E.; Lee, M.; Okuro, K.; Kinbara, K.; Aida, T. High-Water-Content Mouldable Hydrogels by Mixing Clay and a Dendritic Molecular Binder. *Nature* **2010**, *463*, 339−343.

(15) Gong, C.; Liang, J.; Hu, W.; Niu, X.; Ma, S.; Hahn, H. T.; Pei, Q. A Healable, Semitransparent Silver Nanowire−Polymer Composite Conductor. *Adv. Mater.* **2013**, *25*, 4186−4191.

(16) Li, J.; Liang, J.; Li, L.; Ren, F.; Hu, W.; Li, J.; Qi, S.; Pei, Q. Healable Capacitive Touch Screen Sensors Based on Transparent Composite Electrodes Comprising Silver Nanowires and a Furan/Maleimide Diels−Alder Cycloaddition Polymer. *ACS Nano* **2014**, *8*, 12874−12882.

(17) Yu, Z.; Niu, X.; Liu, Z.; Pei, Q. Intrinsically Stretchable Polymer Light-Emitting Devices Using Carbon Nanotube-Polymer Composite Electrodes. *Adv. Mater.* **2011**, *23*, 3989−3994.

(18) Hu, W.; Wang, R.; Lu, Y.; Pei, Q. An elastomeric transparent composite electrode based on copper nanowires and polyurethane. *J. Mater. Chem. C* **2014**, *2*, 1298−1305.

(19) Savagatrup, S.; Printz, A. D.; O'Connor, T. F.; Zaretski, A. V.; Lipomi, D. J. Molecularly Stretchable Electronics. *Chem. Mater.* **2014**, *26*, 3028−3041.

(20) Li, J.; Liang, J.; Jian, X.; Hu, W.; Li, J.; Pei, Q. A Flexible and Transparent Thin Film Heater Based on a Silver Nanowire/Heat-Resistant Polymer Composite. *Macromol. Mater. Eng.* **2014**, *299*, 1403−1409.

(21) Zhu, R.; Chung, C.-H.; Cha, K. C.; Yang, W.; Zheng, Y. B.; Zhou, H.; Song, T.-B.; Chen, C.-C.; Weiss, P. S.; Li, G.; Yang, Y. Fused Silver Nanowires with Metal Oxide Nanoparticles and Organic Polymers for Highly Transparent Conductors. *ACS Nano* **2011**, *5*, 9877−9882.

(22) Gaynor, W.; Burkhard, G. F.; McGehee, M. D.; Peumans, P. Smooth Nanowire/Polymer Composite Transparent Electrodes. *Adv. Mater.* **2011**, *23*, 2905−2910.

(23) Leem, D. S.; Edwards, A.; Faist, M.; Nelson, J.; Bradley, D. D.; de Mello, J. C. Efficient Organic Solar Cells with Solution-Processed Silver Nanowire Electrodes. *Adv. Mater.* **2011**, *23*, 4371−4375.

(24) Kim, Y. H.; Sachse, C.; Machala, M. L.; May, C.; Mueller-Meskamp, L.; Leo, K. Highly Conductive PEDOT:PSS Electrode with Optimized Solvent and Thermal Post-Treatment for ITO-Free Organic Solar Cells. *Adv. Funct. Mater.* **2011**, *21*, 1076−1081.

(25) Lipomi, D. J.; Lee, J. A.; Vosgueritchian, M.; Tee, B. C. K.; Bolander, J. A.; Bao, Z. Electronic Properties of Transparent Conductive Films of PEDOT:PSS on Stretchable Substrates. *Chem. Mater.* **2012**, *24*, 373−382.

(26) Gupta, D.; Wienk, M. M.; Janssen, R. A. J. Efficient Polymer Solar Cells on Opaque Substrates with a Laminated PEDOT:PSS Top Electrode. *Adv. Energy Mater.* **2013**, *3*, 782−787.

(27) Vosgueritchian, M.; Lipomi, D. J.; Bao, Z. Highly Conductive and Transparent PEDOT:PSS Films with a Fluorosurfactant for Stretchable and Flexible Transparent Electrodes. *Adv. Funct. Mater.* **2012**, *22*, 421−428.

(28) Kossmehl, G.; Nagel, H. I.; Pahl, A. Cross-Linking Reactions on Polyamides by Bis(maleimide)s and Tris(maleimide)s. *Angew. Makromol. Chem.* **1995**, *227*, 139−157.

(29) Chen, X. X.; Wudl, F.; Mal, A. K.; Shen, H. B.; Nutt, S. R. New Thermally Remendable Highly Cross-Linked Polymeric Materials. *Macromolecules* **2003**, *36*, 1802−1807.

(30) Lee, J.; Lee, P.; Lee, H. B.; Hong, S.; Lee, I.; Yeo, J.; Lee, S. S.; Kim, T.-S.; Lee, D.; Ko, S. H. Room-Temperature Nanosoldering of a Very Long Metal Nanowire Network by Conducting-Polymer-Assisted Joining for a Flexible Touch-Panel Application. *Adv. Funct. Mater.* **2013**, *23*, 4171−4176.

(31) Xia, Y.; Ouyang, J. PEDOT:PSS Films with Significantly Enhanced Conductivities Induced by Preferential Solvation with Cosolvents and Their Application in Polymer Photovoltaic Cells. *J. Mater. Chem.* **2011**, *21*, 4927−4936.

(32) Xia, Y.; Ouyang, J. Significant Conductivity Enhancement of Conductive Poly(3,4-Ethylenedioxythiophene): Poly-(Styrenesulfonate) Films through a Treatment with Organic Carboxylic Acids and Inorganic Acids. *ACS Appl. Mater. Interfaces* **2010**, *2*, 474−483.

(33) Lim, F. J.; Ananthanarayanan, K.; Luther, J.; Ho, G. W. Influence of a Novel Fluorosurfactant Modified PEDOT:PSS Hole Transport Layer on the Performance of Inverted Organic Solar Cells. *J. Mater. Chem.* **2012**, *22*, 25057−25064.

(34) Huang, H. H.; Ni, X. P.; Loy, G. L.; Chew, C. H.; Tan, K. L.; Loh, F. C.; Deng, J. F.; Xu, G. Q. Photochemical Formation of Silver Nanoparticles in Poly(*N*-Vinylpyrrolidone). *Langmuir* **1996**, *12*, 909−912.

(35) Sun, Y. G.; Yin, Y. D.; Mayers, B. T.; Herricks, T.; Xia, Y. N. Uniform Silver Nanowires Synthesis by Reducing $AgNO_3$ with Ethylene Glycol in the Presence of Seeds and Poly(Vinyl Pyrrolidone). *Chem. Mater.* **2002**, *14*, 4736−4745.

DOI: 10.1021/acsami.5b03482
ACS Appl. Mater. Interfaces 2015, 7, 14140−14149

(36) Wang, J.; Yan, C.; Kang, W.; Lee, P. S. High-Efficiency Transfer of Percolating Nanowire Films for Stretchable and Transparent Photodetectors. *Nanoscale* **2014**, *6*, 10734−10739.

DOI: 10.1021/acsami.5b03482
ACS Appl. Mater. Interfaces 2015, 7, 14140−14149